Critical current measurements in single crystals and single-grain boundaries in $YBa_2Cu_3O_7$ films

by P. Chaudhari
D. Dimos
J. Mannhart

The temperature, magnetic field, and orientation dependence of the critical current density of superconducting $YBa_2Cu_3O_7$ films have been determined from transport measurements. The results support a model of flux creep within single grains and weak-link coupling across grain boundaries.

Introduction

A large number of measurements of the critical current density in the high-temperature superconductors have been made worldwide. All of the measurements show that the critical current density is large in single-crystal samples and substantially smaller in polycrystalline samples. This result is in contrast to that obtained in conventional superconductors, where grain size refinement is one of the most important techniques for enhancing critical current density. To address the issue of low critical current densities and the role that grain boundaries play, we have conducted a series of experiments in which the critical current densities of single-grain boundaries and of their adjacent grains have been directly measured. In this paper, we present a summary of these recent experimental results.

These experiments provide the first direct evidence that grain boundaries are responsible for low critical current densities. We were also able to show that the grain boundaries behave as weak links. In contrast, the critical current density in the single-grain regions appears to be controlled by flux creep. While these measurements were made using thin films of $YBa_2Cu_3O_7$ deposited on $SrTiO_3$, we believe that these findings qualitatively explain the behavior observed in bulk samples. These results also provide insight into the properties of the bismuth- and thallium-based CuO superconductors, which apparently show similar weak-link behavior.

Experimental procedure

To measure the superconducting properties of single grains and grain boundaries it was necessary to 1) produce large-grained samples with well-defined grain-boundary geometries, and 2) develop a technique to pattern the films. To accomplish the first requirement, we prepared bicrystalline or polycrystalline $SrTiO_3$ substrates and subsequently deposited $Y_1Ba_2Cu_3O_{7-\delta}$ films (approximately 1/2 μm thick) by electron-beam evaporation [1]. The films were annealed to produce epitaxial films [2]. The orientation of the substrates is reproduced in the film, so that the film

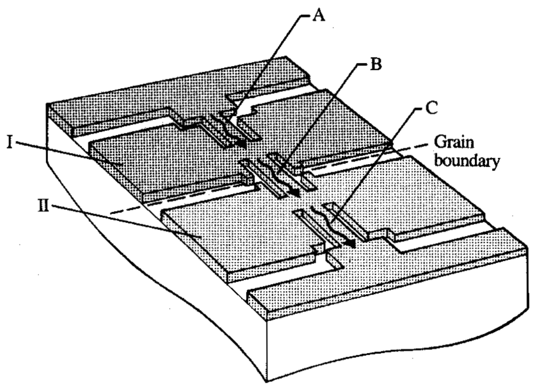

Figure 1

Schematic diagram of the patterned film showing the two grains (regions I and II) and the three narrow lines. Lines A and C are contained entirely within grains I and II, respectively, while line B straddles the grain boundary.

contains grain boundaries as prescribed by the substrates [3–5]. By using the substrate to control the microstructure of the film, large-grained samples of $YBa_2Cu_3O_7$ with well-defined grain-boundary geometries were fabricated.

Following deposition and annealing, the films are patterned with an excimer laser [6] to produce current-carrying lines varying in width from 1–20 μm and in length from 5–100 μm. The lines are patterned across a grain boundary as well as in the two adjoining grains; this situation is shown schematically in **Figure 1**. Electrical leads are attached to the pads on the film by ultrasonically bonding Al wires. Standard four-point, low-frequency measurements were made on these films. A voltage signal of 1–2 μV across the voltage probes was used to define the critical current density.

Critical current density of grains

A number of investigators [1, 7] in different laboratories have shown that the critical current density of epitaxial films can be high (of the order of 10^7 A/cm^2 at 4.2 K). In all of these measurements the current flow is parallel to the Cu–O planes (or perpendicular to the *c*-axis). Because of the high critical current density and the substantial agreement between different investigators, we have used this orientation for most of our work. We have examined a large number of samples, and in the following we summarize our principal findings.

- *Current–voltage curves*

The current–voltage (I–V) characteristics of these films are similar to those of conventional superconductors. A typical example of such an I–V curve, which was obtained at 4.2 K, is shown in **Figure 2(a)**. As illustrated in this figure, once the critical current is exceeded, a smooth, rapid increase in voltage is obtained with increasing current. Due to the nature of the transition, the measured critical current is

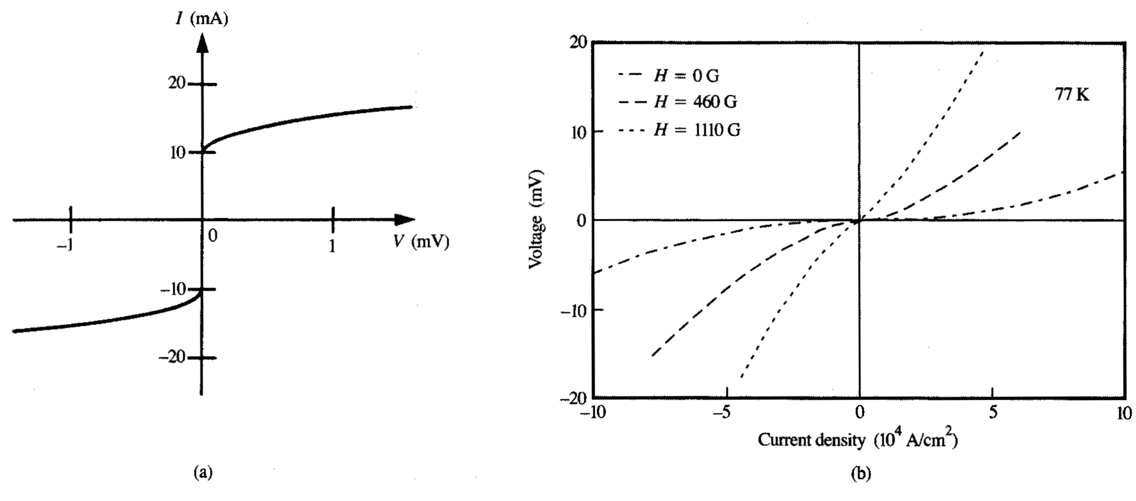

Figure 2

Typical current–voltage characteristics obtained for a narrow line inside a single grain region at (a) 4.2 K and (b) 77 K for fields applied perpendicular to the film.

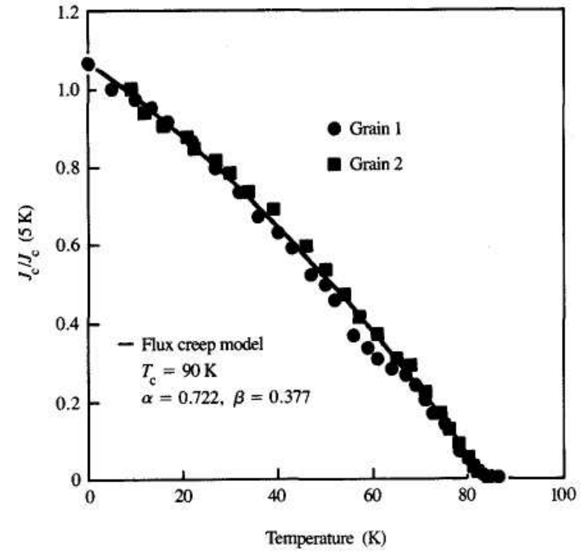

Figure 3

Transport critical current densities (normalized to 5 K values) as a function of temperature for two *c*-axis-normal epitaxial films. The solid line is the fit obtained using the flux creep model. $J_c(0)$ is approximately equal to 6×10^6 A/cm^2 for both grains.

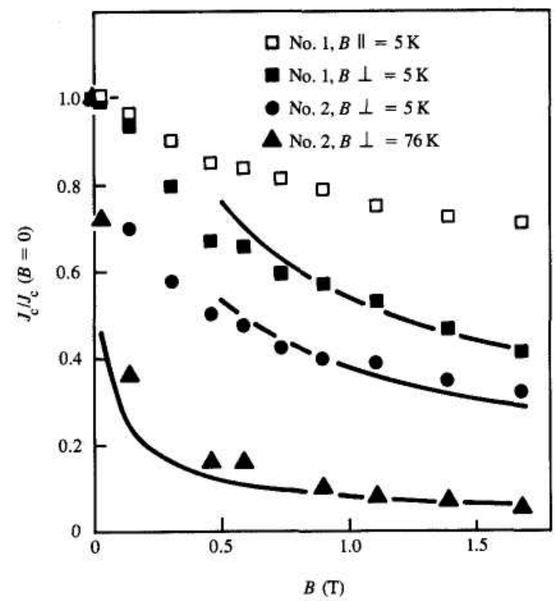

Figure 4

Normalized critical current densities vs. applied field for two samples. The field is oriented perpendicular to or parallel to the plane of the film as indicated, but is always perpendicular to the transport current direction. $J_c(B=0)$ equals 1.3×10^6 and 4.0×10^6 A/cm^2 for samples No. 1 and No. 2, respectively.

relatively insensitive to the exact voltage criteria used. With applied magnetic field, the *I–V* curves tend to straighten out near the origin. This behavior is particularly evident in measurements made at high temperature (close to the transition temperatures). An example of this is shown in **Figure 2(b)**. Again, this type of behavior is in qualitative accord with that of conventional superconductors [8]. We have not attempted to fit a particular theoretical model to the *I–V* curves because of our concern with heating effects.

- *Temperature dependence of the critical current density*

The critical current density of more than 15 samples was measured as a function of temperature. A representative data set is shown in **Figure 3**. The temperature dependence is almost linear except close to the superconducting transition temperature.

Our data can be described quite adequately by a flux creep model, as shown in Figure 3. A number of investigators [9–11] have suggested that the Anderson–Kim creep model [12, 13] may apply to the high-temperature superconductors. Its use in conventional superconductors has been questioned [8, 14]. However, in the high-temperature superconductors it is anticipated that the large temperature range combined with moderate pinning energies may lead to observable creep effects. Experimental evidence in support of a creep model has already been presented in magnetic relaxation studies [15], and our transport data provide additional confirmation.

- *Magnetic field dependence of critical current density*

The critical current density of the films decreases with increasing magnetic field. It decreases faster when the field is perpendicular to the plane of the film than when it is parallel; this effect is shown in **Figure 4**. The drop in critical current density is approximately described by an inverse square root dependence on the applied magnetic field. Such a dependence is consistent with a creep model in which the distance moved by a flux line is set equal to the flux-line lattice parameter [9].

Recent measurements [16] carried out to much higher fields show that the magnetic field dependence initially has the functional dependence shown here. Over the entire range of magnetic field, the dependence is similar to that observed for conventional superconductors and follows their scaling law [14].

- *Orientation dependence of the critical current density*

The critical current density has also been measured as a function of direction within the basal plane. In each of three

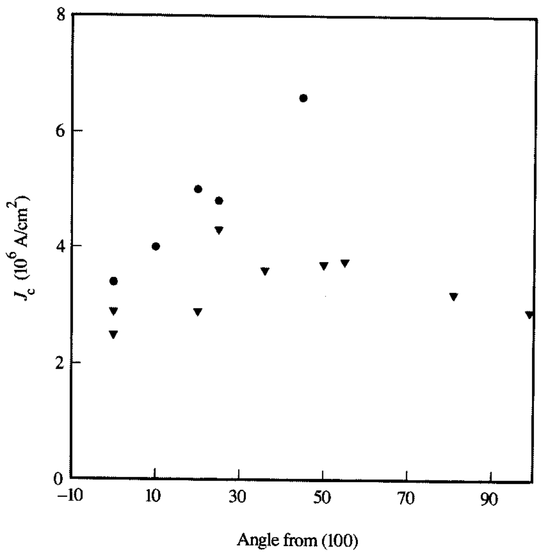

Figure 5

Transport critical current density as a function of direction of current flow within the basal plane. The angle is measured with respect to the (100) or (010) directions.

different samples, a series of patterned lines were made at various angles relative to the $\bar{a}$ (or $\bar{b}$) axis of the film. It should be noted that these directions are macroscopically equivalent due to twinning. Two of the three samples showed a marked orientation dependence, as shown in **Figure 5**, such that the critical current density exhibited a broad maximum when the line was roughly parallel to a [110] direction. In the third sample, no measurable orientation dependence was observed.

The most straightforward explanation of the orientation dependence would be in terms of twins [17, 18]. If these defects provide barriers to the motion of vortices, their well-defined crystallographic and planar arrangement should impose a corresponding crystallographic-dependent critical current density. Another possibility is a variation in the superconductor order parameter with orientation in the plane of the film. A third possibility is that the orientation dependence is due to a deviation in the substrate orientation from the ideal [001] perpendicular one. In this case, decreases in critical current density could be due to a sampling of the out-of-plane component of the critical current density. Unfortunately, our experiments to date cannot differentiate between these possibilities; more work is needed.

- *Vortex pinning*

A number of mechanisms of pinning vortices are possible in superconductors [8]. Within the grains the only two candidates that appear reasonable in the high-temperature superconductors are point defects and twins [17]. Although twins must provide pinning [18], the more important issue is one of determining the dominant pinning center. We believe that the dominant source of pinning is associated with point defects. Vacancies, antisite defects, interstitials, and small defect clusters are all point defects that perturb the order parameter. In materials with a short coherence length [10, 17, 18], point defects can be particularly effective. Vortex decoration data tend to confirm this point of view [19]. Although twins are shown in the decoration technique to be pinning sites, the flux lattice is found to be pinned in the crystal where twins are not present. The pinning of the flux lattice is not associated with any identifiable defect, and it is therefore presumed that the pinning centers are point defects.

- *Summary of grain results*

The temperature dependence of the transport critical current density in the $Y_1Ba_2Cu_3O_{7-\delta}$ films is consistent with flux creep models. The magnetic field dependence is similar to that observed in conventional superconductors. The maximum critical current densities that have been observed in these epitaxial films range from a million to a few million A/cm^2 at 77 K. This value is comparable to that found in conventional superconductors at liquid-helium temperatures, and suggests that many of the applications conceived for the conventional materials are in principle possible with the high-temperature superconductors at the temperature of liquid nitrogen. Alternatively, at helium temperatures the high-temperature superconductors have larger critical current values and hence are superior by this one yardstick.

Critical current density of grain boundaries

Since the discovery of high-temperature superconductors [20], the issue of poor critical current density has haunted their potential for applications. Our initial experiments on epitaxial films, which had relatively high critical currents, demonstrated that the low values obtained in polycrystalline samples were not intrinsic to this class of materials. In addition, there was considerable consensus based on indirect evidence that the relatively low J_c values of the critical current density were due primarily to poor superconducting coupling across grain boundaries. Our measurements of the properties of single-grain boundaries were carried out to address this issue directly.

Initially it was found that the critical current density of single-grain boundaries was always less than the critical current densities of the adjacent single-grain regions. This provided the first direct evidence that grain boundaries indeed are the limiting factor. In addition, a comparison of

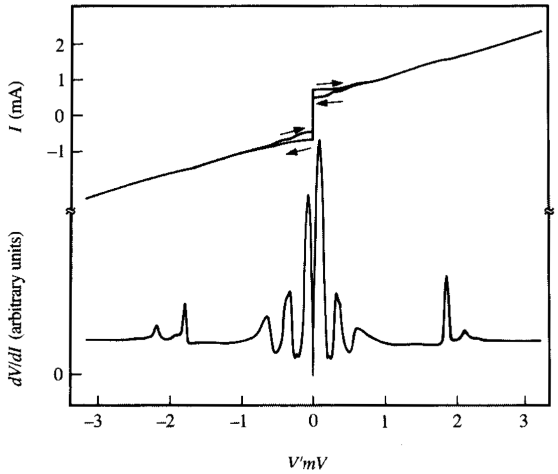

Figure 6

I–V and *dV/dI* characteristics for a typical tilt boundary ($\theta = 37°$) at 5 K.

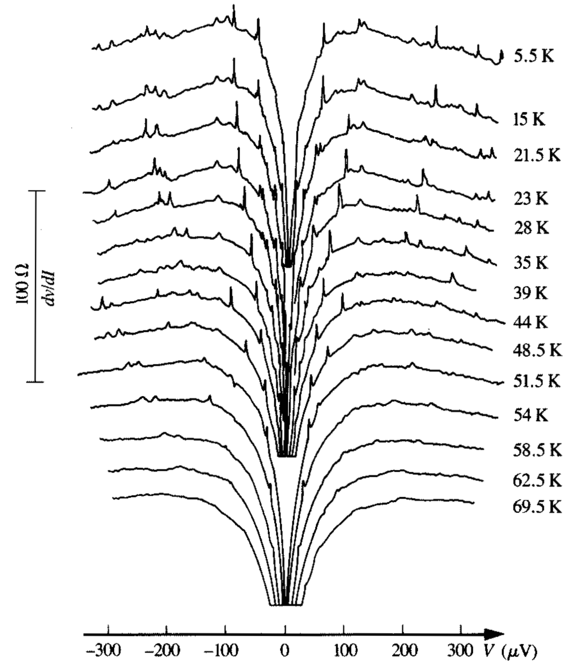

Figure 7

dV/dI vs. *V* for a multi-grained sample at different temperatures with no applied field.

the *I–V* characteristics and the temperature and magnetic field dependence of the critical current density showed that the single-grain boundaries displayed a qualitatively different behavior than the single-grain regions. The characteristics of these grain boundaries are summarized in the following.

• *Current-voltage curves*

The *I–V* curves of the grain boundaries are remarkably different from those of the grains. The onset of finite voltage is abrupt, and the *I–V* curves are approximately linear after that. In addition, we have observed structure at voltages starting at a few tens of microvolts. An example of a typical *I–V* curve is shown in **Figure 6**. The structure is clearly visible in the derivative curve and corresponds to a decrease in conductance. These structures have been found to be present with qualitatively the same features in the *I–V* characteristics of every grain boundary that we have studied. Similar *I–V* curves with such low-voltage structure have been observed in Josephson junctions between conventional superconductors [21].

The location on the voltage scale of these structures varies from boundary to boundary and is found to shift for a given grain boundary on a time scale of some ten minutes. It changes also when the samples are heated above T_c and upon subsequent zero-field cooling. We believe that they reflect resonances in the boundaries, which are controlled by magnetic fields trapped in the boundary or nearby in the grains. The complexity of the *I–V* characteristics of high-T_c materials is therefore expected to increase with the number of grain boundaries per current-carrying line, and indeed, as shown in **Figure 7**, we find a rich structure in a polycrystalline sample containing just a few grain boundaries. **Figure 8** shows the voltage across this sample switching between two states on a millisecond time scale. An increase of the current bias enabled us to observe a sequence of five distinguishable voltage states. The switching in the grain boundary follows a classic chaos pattern. It is conceivable that these features also show up in *I–V* characteristics in experiments designed to obtain tunneling data between polycrystalline samples of high-T_c materials, thus obscuring intrinsic properties of the superconductors.

• *Temperature dependence of critical current density*

The variation of critical current density with temperature was systematically investigated for selected boundaries. The grain boundaries separated crystals whose *c*-axes were parallel but which were rotated relative to each other by a prescribed amount about the *c*-axes. The temperature

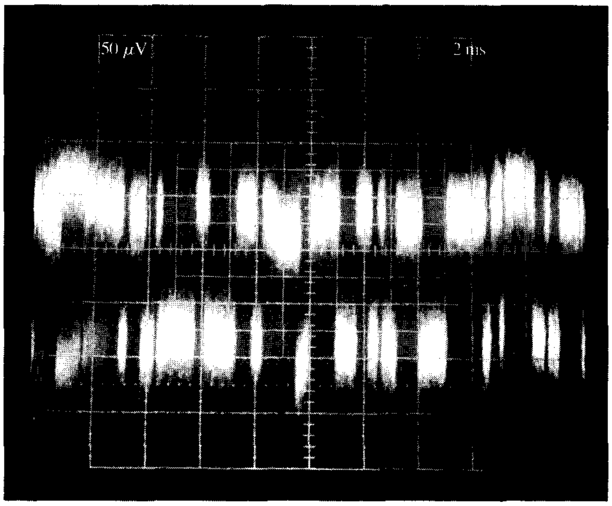

Figure 8

Voltage switching as a function of time for the multi-grained sample.

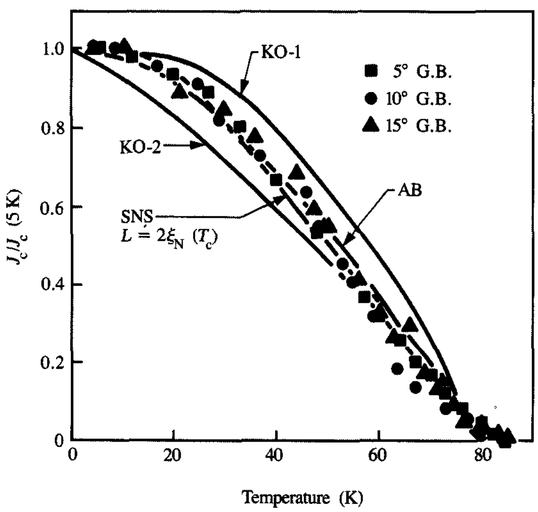

Figure 9

Normalized critical current density as a function of temperature for three grain boundaries with different misorientation angles as indicated. KO-1 and KO-2 are the temperature dependences predicted by Kulik and Omel'yanchuk for weak links in the dirty and clean limits, respectively. The curves labeled AB and SNS refer to the theories of Ambegaokar and Baratoff and of Likharev, respectively. G.B. = grain boundary.

dependence of the critical current density of three different boundaries is shown in **Figure 9**. Although the absolute value of the critical current density was different for the three boundaries, the temperature dependence is, within experimental uncertainty, identical.

Superimposed on the experimental data are some calculated values of the temperature dependence of the Josephson coupling current for several models [22–24], all of which assume that order parameter is suppressed at the grain boundary. The best fit to the data is obtained by using the Ambegaokar–Baratoff (A–B) equation [22] or SNS models in which the normal regions have a thickness comparable to the coherence length of the boundary [23]. However, it should be noted that the measured critical current densities are typically an order of magnitude lower than the values predicted by either model.

• *Magnetic field dependence of critical current density*

The magnetic field dependence of the grain-boundary critical current density provides convincing evidence that the grain boundary behaves as a weak link. The critical current density is observed to be very sensitive to the applied field, as shown in **Figure 10(a)**. For samples in which grain boundaries separate grains with relatively low critical current densities, we find that the magnetic field produces a rich structure **[Figure 10(b)]** reminiscent of inhomogeneous superconductors [25]. The I–V curves, temperature, and magnetic field dependence of the critical current density indicate that the properties of the grain boundaries are dominated by weak coupling.

• *Orientation dependence of the critical current density*

There are several reasons why the superconducting coupling across grain boundaries may be poor in the high-temperature superconductors in comparison with conventional superconductors. One possibility is that the order parameter is severely depressed in the vicinity of a grain boundary because of the structural disorder which is intrinsic to the boundary. In conventional superconductors, where the coherence length is large compared to the width of a grain boundary (1–2 lattice spacings), the coupling across the boundary plane should be strong. However, in the high-T_c oxides, the coherence length is both remarkably short and highly anisotropic. The coherence length in $YBa_2Cu_3O_7$ has been estimated to be about 1–4 Å parallel to the c-axis, which is much shorter than the lattice parameter, and about 15–30 Å parallel to the basal plane. Consequently, a depression in the order parameter at grain boundaries in the high-T_c oxides may be expected [18], and the extent of this depression should depend on the value of the effective coherence length normal to the boundary plane.

Alternatively, the weak-link behavior associated with grain boundaries may arise due to problems in coupling grains of different orientations. The properties associated with the grain boundary should be relatively insensitive to the exact structural nature of the boundary if the poor coupling is due to an intrinsic order-parameter anisotropy. This anisotropy would not only reflect the symmetry of the crystal structure but would also be dependent on the pairing mechanism.

The poorer coupling in the high-T_c materials may be a result of relatively higher grain boundary resistances as compared to those of more conventional superconductors. Measurements on bulk high-T_c samples show that the electrical resistivity is typically more than an order of magnitude larger than for conventional superconductors in the crystalline state. The resistivity is also sensitive to compositional variations, particularly to changes in oxygen concentration. If the stoichiometry at a grain boundary deviates significantly from the bulk, the local resistance may increase. From simple tunneling theory, large boundary resistivities would lead to poor coupling and small supercurrent densities.

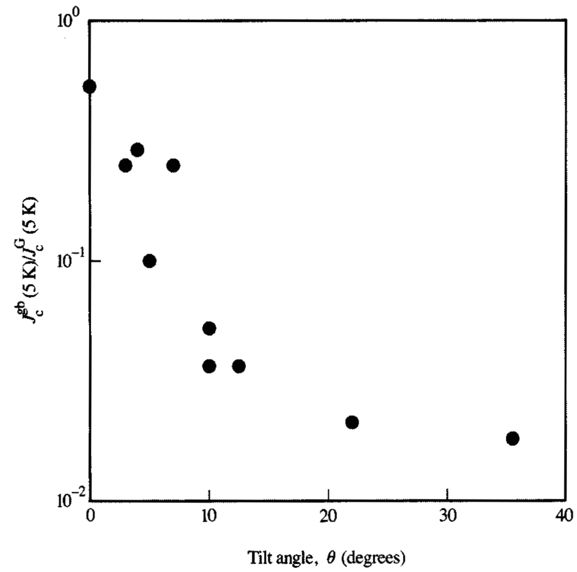

Figure 11

Plot of the ratio of the grain-boundary critical current density to the average value of the critical current density in the two grains at 5 K vs. the misorientation angle in the basal plane.

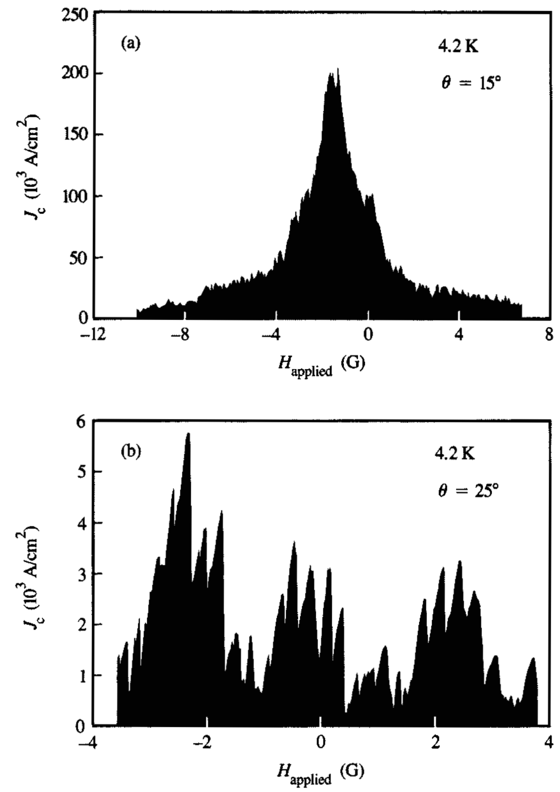

Figure 10

Critical current density as a function of applied field (perpendicular to the film) at 5 K for two different grain boundaries: (a) Typical behavior observed for very homogeneous films with high J_c values. The peak in the curve is equal to the value obtained with zero-field cooling. (b) Typical behavior observed for microstructurally inhomogeneous films with low J_c values.

In order to unravel the mechanisms responsible for the lower critical current density, we are investigating its orientation dependence. Initially, a series of bicrystals was studied in which the misorientation angle is given by rotating one grain relative to another about the *c*-axis. In practice, both grains are rotated about the *c*-axis to yield a symmetrical grain boundary. The current density is found to be a strong function of the misorientation angle, as shown in **Figure 11**. At the present time, we have not been able to establish which of the possibilities discussed above, if any, apply. We are currently collecting data on different orientations which we believe will help in determining the origin of the weak-link behavior.

- *Summary of grain-boundary results*

The *I–V* curves, temperature, and magnetic field dependences of the critical current density of [001] tilt grain boundaries are different from those of grains. The data suggest that these boundaries are weak links and that their behavior compares well with that of superconducting–normal–superconducting Josephson junctions. The critical current density is found to be a strong function of the misorientation angle between the grains. The origin of this behavior is still not understood.

- *Applications of grain boundaries*

The weak-link nature of grain boundaries and the possibility of controlling this phenomenon through predetermined misorientations between grains suggest a number of applications; an obvious one is a SQUID. We have built such a device, and it shows the anticipated variation in current (or voltage) with magnetic field [3]. We have also made some preliminary noise measurements [26], suggesting that SQUID behavior can be further optimized by choosing selected orientations. The noise spectrum can also be a sensitive function of the current bias across the boundary. Interest in developing Josephson device applications using these boundaries indicates that the topic of grain-boundary noise is an interesting area for further study.

References and notes

1. For a description of our evaporation procedure, see P. Chaudhari, R. H. Koch, R. B. Laibowitz, T. R. McGuire, and R. J. Gambino, *Phys. Rev. Lett.* **58,** 2684 (1987) and references cited in this paper.
2. P. Chaudhari, F. LeGoues, and A. Segmuller, *Science* **238,** 342 (1987).
3. P. Chaudhari, J. Mannhart, D. Dimos, C. C. Tsuei, J. Chi, M. M. Oprysko, and M. Scheuermann, *Phys. Rev. Lett.* **60,** 1653 (1988).
4. D. Dimos, P. Chaudhari, J. Mannhart, and F. K. LeGoues, *Phys. Rev. Lett.* **61,** 219 (1988).
5. J. Mannhart, P. Chaudhari, D. Dimos, C. C. Tsuei, and T. R. McGuire, *Phys. Rev. Lett.* **61,** 2476 (1988).
6. J. Mannhart, M. Scheuermann, C. C. Tsuei, M. M. Oprysko, C. C. Chi, C. P. Umbach, R. Koch, and C. Miller, *Appl. Phys. Lett.* **52,** 1271 (1988).
7. There are many laboratories that produce high-critical-current-density films. Some of the early work was reported by Oh et al., *Appl. Phys. Lett.* **51,** 852 (1987) and Enomoto et al., *Jpn. J. Appl. Phys.* **26,** L1248 (1987). Some of the highest values at 77 K have been reported by Roas et al., *Appl. Phys. Lett.* **53,** 1567 (1988) and Dam et al., preprint.
8. A. M. Campbell and J. E. Evetts, *Adv. Phys.* **21,** 199 (1972).
9. D. Dew-Hughes, preprint.
10. M. Tinkham, *Helv. Phys. Acta* **61,** 443 (1988).
11. P. H. Kes, preprint.
12. P. W. Anderson, *Phys. Rev. Lett.* **9,** 309 (1962).
13. Y. B. Kim, *Rev. Mod. Phys.* **36,** 39 (1964).
14. E. J. Kramer, *J. Electron. Mater.* **4,** 839 (1975).
15. Y. Yeshurun and A. P. Malozemoff, *Phys. Rev. Lett.* **60,** 2202 (1988).
16. J. S. Satchell, R. G. Humphreys, N. G. Chew, J. A. Edwards, and M. J. Kane, *Nature* **334,** 331 (1988).
17. P. Chaudhari, *Jpn. J. Appl. Phys.* **26,** 2023 (1987).
18. G. Deutscher and K. A. Mueller, *Phys. Rev. Lett.* **59,** 1745 (1987).
19. G. J. Dolan, G. V. Chandresekhar, T. R. Dinger, C. Feild, and F. Holtzberg, preprint.
20. J. G. Bednorz and K. A. Müller, *Z. Phys. B* **64,** 198 (1986).
21. J. Clarke, *Phys. Rev. B* **4,** 2963 (1971); G. M. Daalmans, T. M. Klapwijk, and J. E. Mooij, *IEEE Trans. Magnetics* **13,** 719 (1977).
22. V. Ambegaokar and A. Baratoff, *Phys. Rev. Lett.* **10,** 486 (1963) and **11,** 104(E) (1963).
23. K. K. Likharev, *Rev. Mod. Phys.* **51,** 101 (1979).
24. I. O. Kulik and A. N. Omel'yanchuk, *Fiz. Nizk. Temp.* **3,** 945 (1977) [*Sov. J. Low Temp. Phys.* **3,** 459 (1977)].
25. P. K. Hansma and J. R. Kirtley, *J. Appl. Phys.* **45,** 4016 (1974).
26. A. I. Braginski, M. G. Forrester, J. Talvacchio, and G. R. Wagner, *Proceedings of the 5th International Workshop on Future Electron Devices*, Miyagi-Zao, 1988, pp. 171–179.

Received February 8, 1989; accepted for publication February 16, 1989

Praveen Chaudhari *IBM Research Division, T. J. Watson Research Center, P.O. Box 218, Yorktown Heights, New York 10598.*

Dr. Chaudhari obtained a B.S.(Honors) from the Indian Institute of Technology (1961), and an M.S. (1963) and a Sc.D (1966), both in physical metallurgy, from the Massachusetts Institute of Technology, Cambridge. Since joining the T. J. Watson Research Center as a Research Staff Member in 1966, he has held various management responsibilities in science and science-related technologies such as optical storage, magnetic bubbles, and the Josephson program. He was appointed Director of the Physical Sciences Department in 1981, Vice-President for Science and Technology, IBM Research Division, in 1982, and a member of the Corporate Technical Committee in 1989. Dr. Chaudhari has worked on the structure and properties of amorphous solids, mechanical properties of thin films, defects in solids, quantum transport in disordered systems, superconductivity, and on the magnetic monopole and neutrino mass experiments. He has several IBM awards, and was the first recipient of the Leadership Award (1986) of the Metallurgical Society of AIME for his contributions to advancing the science and technology of electronic materials. He received the George E. Pake Award of the American Physical Society (1987) for his personal contributions to science and management of science. Dr. Chaudhari is a member of the American Association for the Advancement of Science, the American Institute of Mining, Metallurgical and Petroleum Engineers, and the National Academy of Engineering. He is a Fellow of the American Physical Society.

Duane Dimos *IBM Research Division, T. J. Watson Research Center, P.O. Box 218, Yorktown Heights, New York 10598.*

Dr. Dimos received a B.A. in physics from the University of California at Berkeley in 1980. He received an M.S. and Ph.D. in materials science from Cornell University in 1982 and 1986, respectively. Dr. Dimos joined IBM in 1987 as a postdoctoral research associate in the Materials Science group.

Jochen Mannhart *Universität Tübingen, Physikalisches Institut, Morgenstelle 14 D-7400, Tübingen, Federal Republic of Germany.*

Dr. Mannhart received his Ph.D. from the University of Tübingen in 1987. He was on the research staff of the IBM T. J. Watson Research Center as a visiting scientist from 1987 to 1989. He has worked in the fields of Josephson tunnel junctions and low-temperature scanning electron microscopy. His present interests center upon the transport properties of high-T_c films. Dr. Mannhart is a member of the German Physical Society.